

# On Explosion Limits of Ammonia–Oxygen Mixtures with Hydrogen Addition: Sensitivity and Nonmonotonicity

Cheng Zhou, Wenkai Liang,\* and Zheng Chen

Cite This: *Energy Fuels* 2021, 35, 14035–14041

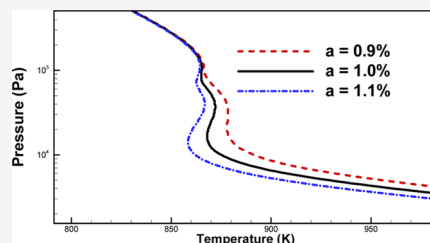
Read Online

ACCESS |

Metrics & More

Article Recommendations

**ABSTRACT:** We investigate numerically the ammonia–hydrogen–oxygen explosion limits, showing that the addition of a trace amount of hydrogen to ammonia–oxygen mixtures can qualitatively modify the explosion limits from the monotonic case to the nonmonotonic case, with multiple turning points including being Z-shaped which is characteristic of hydrogen–oxygen explosions. Furthermore, as the hydrogen concentration increases, (1) the first limit moves toward lower temperature conditions; (2) the second limit also shifts toward lower temperature conditions when the hydrogen addition is less than 10% of the ammonia–hydrogen fuel, but it moves in the opposite direction with higher additions; and (3) the third limit is minimally affected. Sensitivity analysis shows that at different pressures, the dominant reactions change with hydrogen addition. The present results facilitate understanding of the kinetic interaction between hydrogen and ammonia and are of practical relevance to the safe handling of ammonia–hydrogen fuels.



## 1. INTRODUCTION

As an essential alternative fuel for achieving zero-carbon emissions and carrying hydrogen, ammonia has recently drawn much attention for its potential usage in transportation and industrial processes.<sup>1,2</sup> It can be produced through renewable electricity with reactions between hydrogen and nitrogen. For its usage in energy conversion, it can be either converted to hydrogen or directly utilized in solid oxide fuel cells and combustion systems. For combustion applications, however, ammonia has several limitations such as lower flame speeds, longer ignition delay times, and narrower flammability limits<sup>1,2</sup> compared with other commonly used fuels. To overcome these obstacles, ammonia has been blended with hydrogen, methane, or syngas to enhance its reactivity. Consequently, studies have been conducted<sup>3–8</sup> toward determining the fundamental combustion parameters mentioned above and understand the fundamental kinetics of ammonia and ammonia-based fuel blends. For example, laminar premixed flames of ammonia,<sup>3</sup> ammonia–methane,<sup>4</sup> and ammonia–hydrogen<sup>5</sup> have been investigated experimentally; detailed and reduced kinetic models of ammonia–hydrogen–methane mixtures have been developed;<sup>6</sup> and the ignition characteristics<sup>7</sup> and NO<sub>x</sub> formation<sup>8</sup> of ammonia–hydrogen mixtures have also been studied. Recently, the ammonia oxidation and pyrolysis kinetics has been investigated in a jet stirred flow reactor (JSFR),<sup>9–11</sup> and the importance of third-body efficiencies in ammonia–hydrogen blend kinetics has been discussed in ref 12. It is essential to note that, at higher pressures, several third-body reactions involving both H- and N-containing species are important for the accurate prediction of ammonia and ammonia-blend fuel oxidation. Furthermore, a very recent

study<sup>13</sup> has investigated the explosion limits of NH<sub>3</sub>–H<sub>2</sub>–O<sub>2</sub> using sensitivity analysis and eigenvalue analysis. The current work aims at demonstrating the pressure–temperature explosion boundary of ammonia–hydrogen–oxygen at relatively low concentrations of hydrogen and also explains how the monotonic ammonia–oxygen explosion limits transition to the classical nonmonotonic, Z-shaped curve of hydrogen–oxygen mixtures when adding in different amounts of hydrogen.

The present study is motivated by identifying the effects of hydrogen addition on the explosion limits of NH<sub>3</sub>–O<sub>2</sub> mixtures, particularly on its sensitivity in affecting the limits from being monotonic to Z-shaped. Indeed, we shall show in due course that the sensitivity can be considered to be “catalytic” in nature, in that only a trace amount of hydrogen addition is needed to affect the qualitative nature of the limit curve. This sensitivity not only is essential in understanding the overall kinetics but is also relevant for safety considerations in transportation and storage.

We note in passing that recent studies on the addition of a secondary reactant to the well-studied hydrogen–oxygen system,<sup>14</sup> such as carbon monoxide<sup>15</sup> and methane<sup>16</sup> as secondary fuels and NO<sup>17</sup> and O<sub>3</sub><sup>18</sup> as secondary oxidizers,

Received: June 2, 2021

Revised: August 10, 2021

Published: August 20, 2021



have revealed substantial modifications of the characteristic Z-shaped response and demonstrated the richness of the underlying kinetics of reacting mixtures involving hydrogen as a reactant. Furthermore, in practice, the understanding of ammonia and ammonia–hydrogen explosion limits is essential for the safe handling of ammonia and ammonia–hydrogen binary fuel for their transportation and storage. Also, it is relevant to the understanding of engine knocking using ammonia or ammonia-based blend fuels.

In the following sections, we will first present the numerical methodology and discuss the kinetic model selections. Then, the global response of ammonia–hydrogen–oxygen explosion limits with different hydrogen-to-ammonia ratios will be investigated, demonstrating that only a trace amount of hydrogen addition is needed to affect the transition to complex nonmonotonicity. This will be followed by local and detailed kinetic analyses of the explosion limits under different pressure–temperature conditions.

## 2. METHODOLOGY

The simulation used the SENKIN code<sup>19</sup> to compute the explosive and nonexplosive boundary of  $\text{NH}_3\text{--H}_2\text{--O}_2$  mixtures. The SENKIN code has been widely used in the combustion community for computing the time evolution of temperature, pressure, and chemical species in a closed system. It solves a set of nonlinear ordinary differential equations with the given initial values of a homogeneous reacting gas mixture. The criterion of explosion is set as running the reactor simulation for 10 s to observe more than 50 K temperature change in the end. The ranges of initial pressure and temperature have been selected as  $3.5$  to  $6 \times 10^8$  Pa and 300–2500 K, respectively. Several kinetic models were assessed, as will be discussed in the following. Wall termination reactions<sup>20</sup> for active species such as H and  $\text{NH}_2$  were considered with a temperature-dependent reaction rate.<sup>14</sup>

In the following discussions, the equivalence ratio is fixed at unity considering both hydrogen and ammonia as the fuel. The molar ratio for  $\text{NH}_3/\text{H}_2/\text{O}_2$  is  $(1 - a)/a/(0.75 - 0.25a)$ , where  $a$  is the fraction of hydrogen in the binary ammonia–hydrogen mixtures. For the current work, we focus on the situation of ammonia–hydrogen–oxygen mixtures without any diluent. However, the additions of diluents such as  $\text{N}_2$  and  $\text{CO}_2$  will lead to additional thermal and kinetic effects such as changing the temperature evolution and the third-body reaction rates, which are worthy of future studies.

## 3. RESULTS AND DISCUSSION

**3.1. Comparison of Kinetic Models.** To validate and assess the validity of different kinetic models for the ammonia–hydrogen binary fuels, we have compared the results from several detailed mechanisms. Following the experimental cases in ref 21, we consider the  $\text{NH}_3\text{--H}_2\text{--air}$  mixtures with the hydrogen fraction  $a = 0.50 \equiv 50\%$ , equivalence ratio varying from 0.5 to 2.0, and initial pressures of 1.4, 11, and 30 atm. Four recently published mechanisms, respectively, by Otomo et al.,<sup>21</sup> Glarborg et al.,<sup>22</sup> Mei et al.,<sup>23</sup> and Nakamura et al.,<sup>24</sup> were used. These selected models represent the current knowledge of ammonia kinetics, but the uncertainty is inevitable in these kinetic models. The uncertainties in the ammonia kinetics have been analyzed recently using the adjoint sensitivity analysis,<sup>25</sup> which indicates both the importance of accurate kinetic parameters and

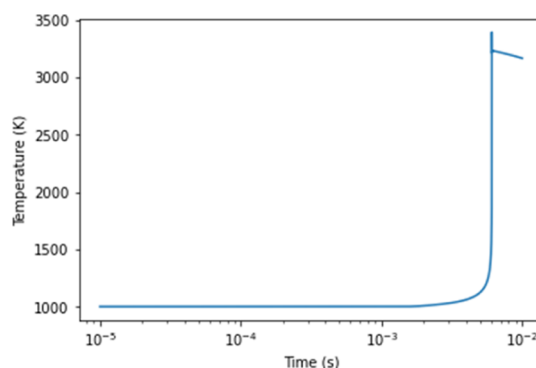


**Figure 1.** Temperature profile during ignition for stoichiometric  $\text{NH}_3\text{--H}_2\text{--O}_2$  mixtures (hydrogen fraction,  $a = 10\%$ ) at  $P = 1$  atm and  $T = 1000$  K.

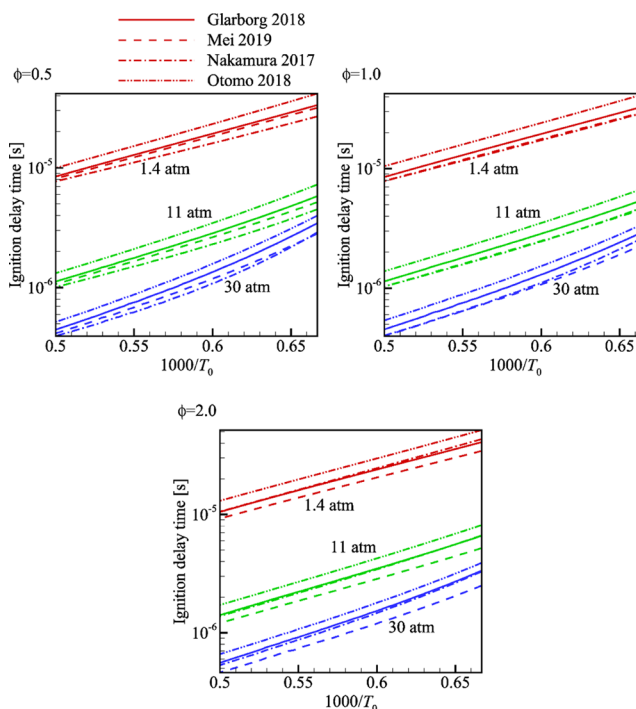


**Figure 2.** Ignition delay times for  $\text{NH}_3\text{--H}_2\text{--air}$  (hydrogen fraction,  $a = 50\%$ ) at different equivalence ratios and pressures.

thermal data for the predictions of ammonia combustion. Figure 1 demonstrates the typical temperature profile using the Glarborg mechanism, which shows that the temperature has a sudden increase at the ignition timing and then exhibits a slight decrease due to the radical terminations at wall. Furthermore, it is worth noting that the temperature change at ignition is normally very sharp; hence, the criterion for determining explosion is not very sensitive to the temperature increase (50 K increase has been used in this work). Figure 2 shows that the ignition timings predicted by the selected mechanisms behave similarly.

While the performance of these models behaves similarly in predicting the ignition timings, they could yield substantially different responses to pressure–temperature variations in the explosion limits. Figure 3 plots the explosion boundaries of stoichiometric  $\text{NH}_3\text{--H}_2\text{--O}_2$  mixtures predicted by these selected kinetic models, showing the obvious trend that the mixture becomes more explosive at higher hydrogen fractions when the fuel composition transitions from  $\text{NH}_3$  to  $\text{H}_2$ . More

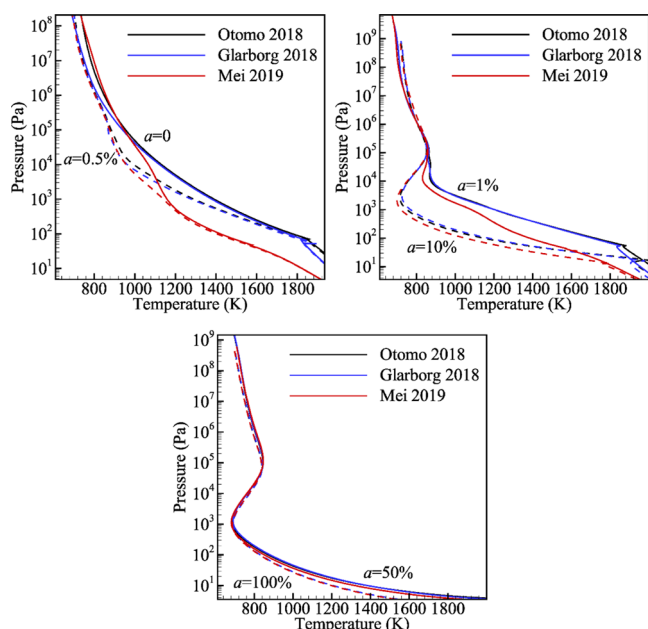


**Figure 3.** Explosion boundaries of stoichiometric  $\text{NH}_3\text{-H}_2\text{-O}_2$  mixtures predicted by several kinetic models.

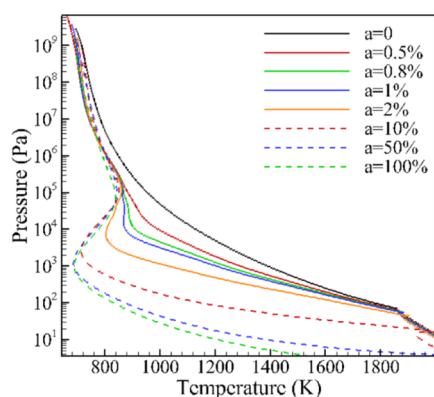


**Figure 4.** Explosion boundaries of  $\text{NH}_3\text{-H}_2\text{-O}_2$  mixtures with the hydrogen fraction varying from 0 to 1.

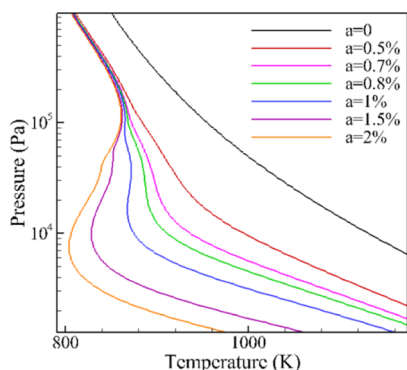


**Figure 5.** Explosion limits of  $\text{NH}_3\text{-H}_2\text{-O}_2$  mixtures near the monotonic to nonmonotonic transition.

specifically, in the model used in the detailed study, we first note that since the model of Nakamura et al.<sup>24</sup> was designed for weak flame simulations, it could not predict the explosion limits. Next, the results can be predicted consistently by the models of Otomo et al.<sup>21</sup> and Glarborg et al.,<sup>22</sup> while that of

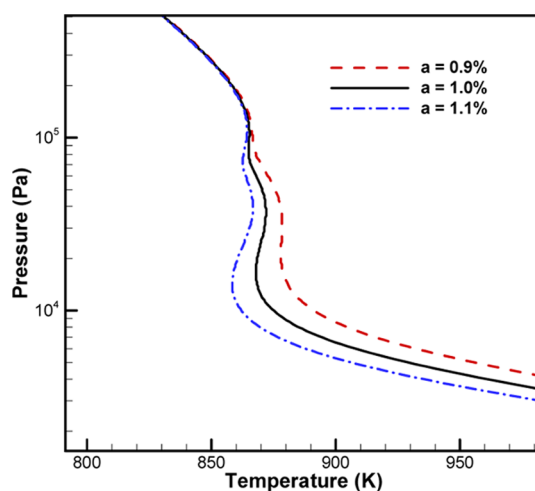


**Figure 6.** Evolution of multiple turnings in the nonmonotonic explosion limits of  $\text{NH}_3\text{-H}_2\text{-O}_2$  mixtures.

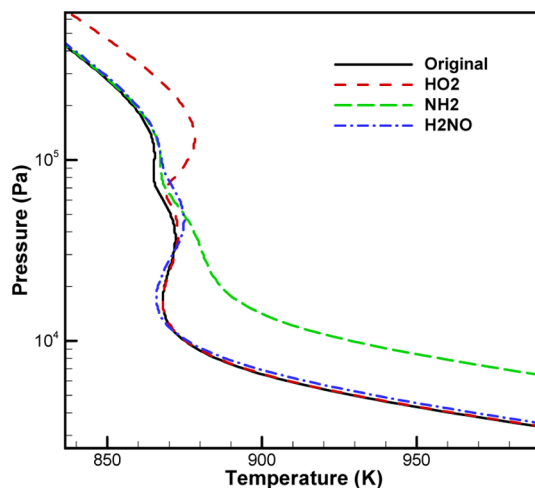


**Figure 7.** Explosion boundaries of  $\text{NH}_3\text{-H}_2\text{-O}_2$  mixtures with wall termination reactions perturbed at hydrogen fraction  $a = 1\%$ .

Mei et al.<sup>23</sup> has different results for low hydrogen fractions of  $a = 0.5$  and  $1\%$ , especially at lower pressures. Furthermore, the differences are relatively large for  $a \leq 1\%$  for which the controlling kinetics is dominated by the  $\text{NH}_3$  oxidation reactions. By also noting that the model of Otomo et al.<sup>21</sup> has good performance in predicting the laminar flame speeds and ignition delay times over a wide span of equivalence ratios and pressures, in the following studies, we shall use this model, which has 32 species and 213 reactions.

**3.2. Global Behavior of Explosion Limits.** Results of the explosion limits with different amounts of  $\text{H}_2$  are demonstrated in Figure 4. The hydrogen fraction,  $a$ , changes from zero to unity, indicating the progression of the compositions from the  $\text{NH}_3\text{-O}_2$  mixture to the  $\text{H}_2\text{-O}_2$  mixture, with the global mixture equivalence ratio set to unity. It is worth noting that as  $\text{H}_2$  addition increases, the low-pressure, first limit continuously moves toward the lower temperature side and the higher-pressure second limit also shifts to lower temperature conditions, but then shifts back very slightly to the higher temperature conditions as  $a$  changes from 10 to 100%. The very high-pressure, third limit almost remains unaffected, while it still demonstrates a similar trend to that of the second limit.

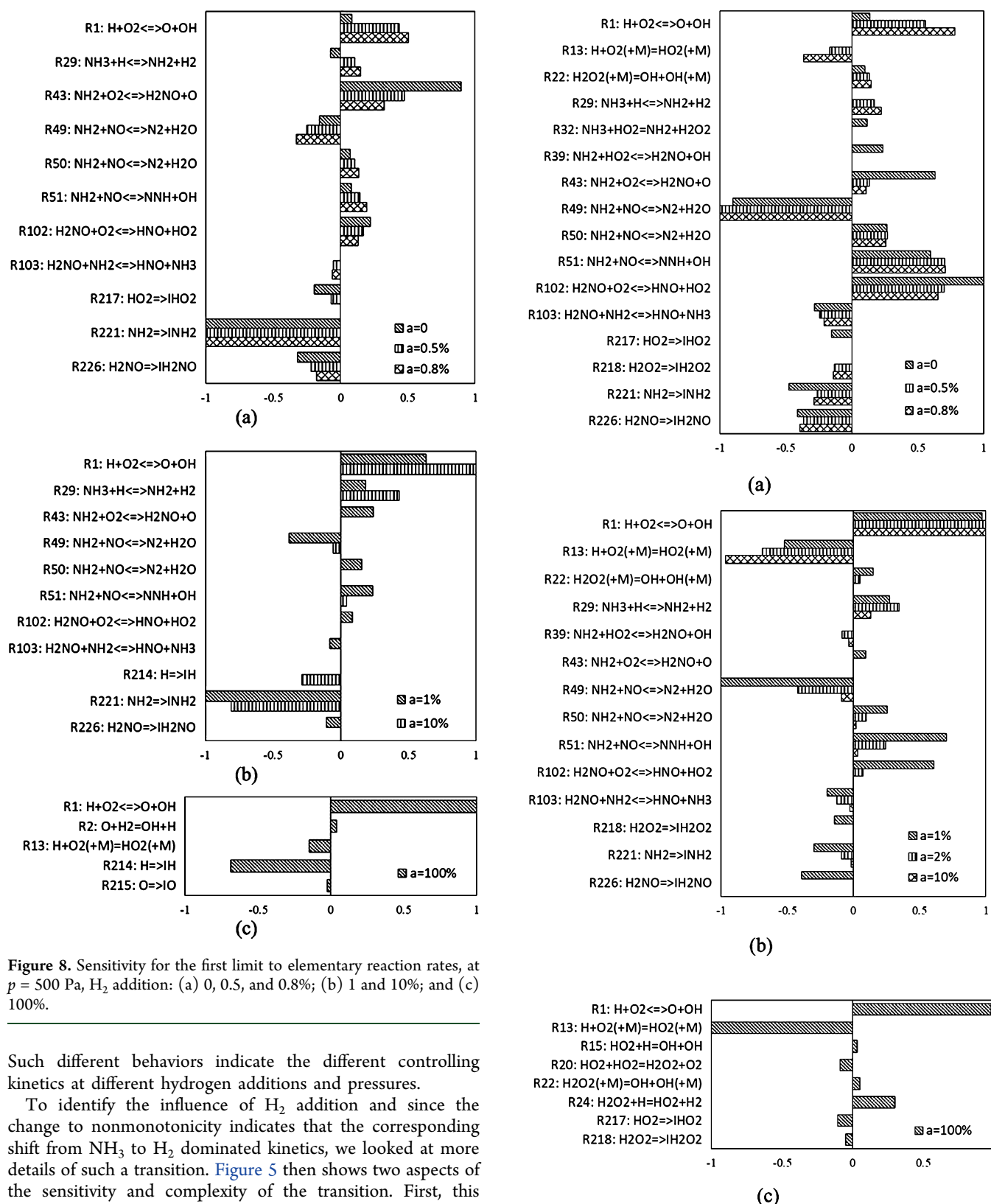


**Figure 8.** Sensitivity for the first limit to elementary reaction rates, at  $p = 500$  Pa,  $H_2$  addition: (a) 0, 0.5, and 0.8%; (b) 1 and 10%; and (c) 100%.

Such different behaviors indicate the different controlling kinetics at different hydrogen additions and pressures.

To identify the influence of  $H_2$  addition and since the change to nonmonotonicity indicates that the corresponding shift from  $NH_3$  to  $H_2$  dominated kinetics, we looked at more details of such a transition. Figure 5 then shows two aspects of the sensitivity and complexity of the transition. First, this transition for  $NH_3-H_2-O_2$  mixtures occurs around the very small amount of addition of  $a = 0.01$  or 1%. Also, the transition happens under low-pressure conditions, where the first and second limits of the explosion limits are found to be sensitive to hydrogen addition.

The second aspect is that upon close examination, the transition boundary of  $a = 1\%$  actually consists of four turning points instead of the two turning points characteristic of the Z-

**Figure 9.** Sensitivity analysis for the second limit to elementary reaction rates, at  $p = 30,000$  Pa,  $H_2$  addition: (a) 0, 0.5, and 0.8%; (b) 1, 2, and 10%; and (c) 100%.

curve. To further demonstrate the nature of the transition, Figure 6 resolves the explosion responses from  $a = 0.8$  to 1.1%. It is then of interest to note that the transition evolves from

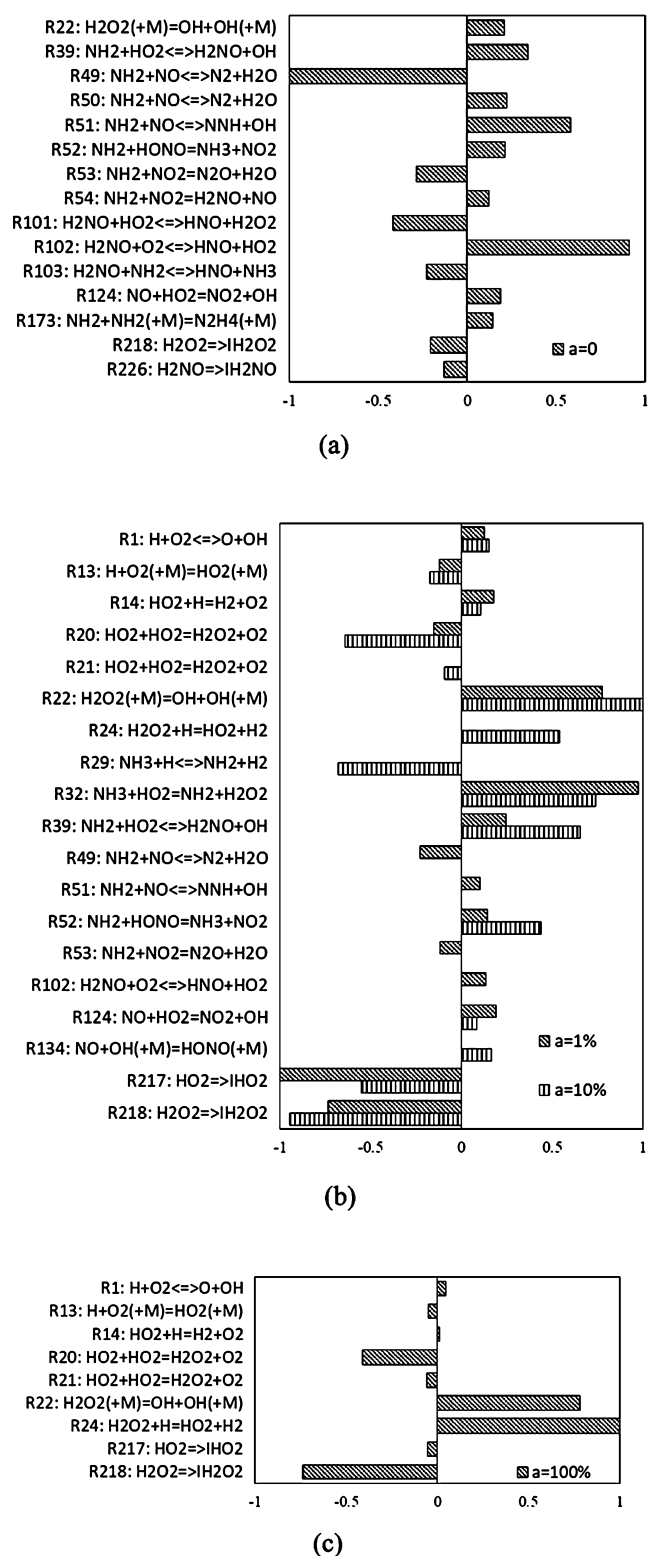


**Figure 10.** Sensitivity analysis of the third limit to elementary reaction rates, at  $p = 1 \times 10^6$  Pa,  $H_2$  addition: (a) 0; (b) 1 and 10%; and (c) 100%.

being monotonic to the one with two turning points and then to the one with four turning points. With yet higher hydrogen addition, Figure 5 shows that the explosion reverts back to the characteristic Z-curve of three limits with two turning points, demonstrating the dominant and sensitive role of hydrogen.

In order to quantify the effect of wall termination reactions, we have performed the sensitivity analysis of wall terminating reactions by perturbing the rate coefficients (multiplying the original rate by a factor of 2), as demonstrated in Figure 7. The wall termination of  $HO_2$  is essential for high-pressure conditions, while those of  $NH_2$  and  $H_2NO$  are important for relatively lower pressures.

Next, the detailed kinetics for the explosion of  $NH_3-H_2-O_2$  mixtures will be further studied.

**3.3. Detailed Kinetic Analysis.** To quantify the detailed kinetics, the sensitivity analysis of several typical pressures of the three-limit Z-curve strongly affected by hydrogen–oxygen chemistry will be performed and discussed. For every  $H_2$  level, one temperature condition will be selected on the explosive side of the boundary.

The low-pressure, first explosion limit for  $NH_3-O_2$  is dominated by R43:  $NH_2 + O_2 = H_2NO + O$  and wall termination of  $NH_2$  (R221), as seen in the  $a = 0$  case in Figure 8a. As  $H_2$  is added, the large amount of active H radical promotes chain branching reactions such as R1:  $H + O_2 = O + OH$ , and also, the H atom reacts with  $NH_3$  to produce the active intermediate  $NH_2$  through R29:  $NH_3 + H = NH_2 + H_2$ , which increases the global reactivity. This accounts for the significant transition of this limit toward the lower pressure and temperature conditions. Since more  $NH_2$  is produced, the  $NH_2$ -related reactions, for example, R49–R51, start to be more important, as shown in Figure 8b. Since the H atom participates in the process of  $O_2$  consumption through R1:  $H + O_2 = O + OH$ , competing with  $NH_2$ , this leads to the decline in the significance of R43:  $NH_2 + O_2 = H_2NO + O$ , producing less  $H_2NO$ , and hence, the  $H_2NO$ -related reactions (such as R120 and R226) become less important.

With continuously increasing  $H_2$  concentration, H atoms instead of  $NH_2$ -related reactions gradually dominate, until the response degenerates to that dominated by the pure hydrogen–oxygen reactions, as shown in Figure 8c.

Next, the second limit with different amounts of  $H_2$  addition will be investigated. At intermediate pressures, as Figure 9 shows, for the pure  $NH_3$ –air mixture, R102:  $H_2NO + O_2 = HNO + H_2O_2$  and R51:  $NH_2 + H_2 = NNH + OH$  promote combustion the most, due to the active OH radical and HNO produced, while R49:  $NH_2 + H_2 = N_2 + H_2O$  inhibits the process the most, due to the stable products of  $N_2$  and  $H_2O$ . As more  $H_2$  is added, the H atom rapidly dominates the ignition process, with it consuming  $O_2$  to produce the OH radical, and reduces the extent of  $H_2NO$  reacting with  $O_2$ . As seen in the cases for  $a$  varying from 0.5 to 2%, the significance of R1:  $H + O_2 = O + OH$  increases substantially and the sensitivity of R102:  $H_2NO + O_2 = HNO + H_2O_2$  decreases, and  $O_2$  is consumed mainly by the H atom rather than  $H_2NO$  for  $a > 0.5\%$ . For all these five cases, the OH radical production reaction R51:  $NH_2 + H_2 = NNH + OH$  promotes combustion the most, while the chain termination reaction R49:  $NH_2 + H_2 = N_2 + H_2O$  is the dominant inhibiting reaction.

As the hydrogen addition continuously increases, the H-atom-related reactions further dominate. The competition of the H radical between R1 and R13 shows the typical behavior of the second limit of the  $H_2-O_2$  mixture, as discussed in ref 14. Compared to pure hydrogen–oxygen mixtures, the second limit for the mixture with relatively less reactive  $NH_3$  moves to the high-temperature and high-pressure side.

For the high-pressure cases, as Figure 10 shows, the third limit is mainly determined by the  $\text{HO}_2^-$  and  $\text{H}_2\text{O}_2$ -related reactions of  $\text{HO}_2 + \text{HO}_2 = \text{H}_2\text{O}_2 + \text{O}_2$ ,  $\text{H}_2\text{O}_2 (+\text{M}) = \text{OH} + \text{OH} (+\text{M})$  and  $\text{H}_2\text{O}_2 + \text{H} = \text{HO}_2 + \text{H}_2$ . Meanwhile, the reactive  $\text{NH}_2$  would promote the reaction through  $\text{NH}_2 + \text{HO}_2 = \text{H}_2\text{NO} + \text{OH}$ , which counteracts with OH radical depletion by  $\text{NH}_3 + \text{OH} = \text{NH}_2 + \text{H}_2\text{O}$  and  $\text{NH}_2 + \text{OH} = \text{NH} + \text{H}_2\text{O}$ . Thus, the third limit does not change much as the hydrogen ratio changes.

#### 4. CONCLUSIONS

The monotonic pressure–temperature explosion limit curve of ammonia–oxygen mixtures rapidly changes to the non-monotonic Z-shaped limit curve, characteristic of hydrogen–oxygen mixtures, with only a minute amount of hydrogen addition to ammonia. In terms of the response to increasing hydrogen addition at each of these three limits, it is shown that the first limit keeps changing and then saturates with increasing  $\text{H}_2$  adding in; the second limit shows a monotonic to nonmonotonic variation; and the third limit exhibits almost no shift due to  $\text{H}_2$  addition.

Further analysis has shown that the first limit is governed by the  $\text{H}_2$ -related reactions and shifts to lower temperatures/pressures with  $\text{H}_2$  adding in. Then, at the second limit, without  $\text{H}_2$  addition,  $\text{NH}_2^-$  and  $\text{H}_2\text{NO}$ -related reactions are essential and the consequence is the enhanced OH production. With  $\text{H}_2$  addition, the H atom rapidly dominates the OH production, leading to the formation of the stable products  $\text{N}_2$  and  $\text{H}_2\text{O}$ . The nonmonotonic variations of the second limit are due to this competing effect. The  $\text{HO}_2$  and  $\text{H}_2\text{O}_2$  chemistry is important for the third limit, and as such, it does not change much as the hydrogen ratio changes.

The multiple, four-turning-point response around  $a = 1\%$  appears to be rather restrictive in its manifestation in terms of the limited range of hydrogen addition yet nevertheless merits further study for its potential fundamental and practical significance.

#### AUTHOR INFORMATION

##### Corresponding Author

Wenkai Liang – Department of Mechanical and Aerospace Engineering, Princeton University, Princeton, New Jersey 08544, United States; [orcid.org/0000-0002-8086-1155](https://orcid.org/0000-0002-8086-1155); Email: [wenkail@princeton.edu](mailto:wenkail@princeton.edu)

##### Authors

Cheng Zhou – Center for Combustion Energy, and Department of Energy and Power Engineering, Tsinghua University, Beijing 100084, China

Zheng Chen – SKLTCs, HEDPS, CAPT, College of Engineering, Peking University, Beijing 100871, China; [orcid.org/0000-0001-7341-6099](https://orcid.org/0000-0001-7341-6099)

Complete contact information is available at:

<https://pubs.acs.org/10.1021/acs.energyfuels.1c01764>

##### Notes

The authors declare no competing financial interest.

#### REFERENCES

- (1) Kobayashi, H.; Hayakawa, A.; Somarathne, K. D. K. A.; Okafor, E. C. Science and technology of ammonia combustion. *Proc. Combust. Inst.* **2019**, *37*, 109–133.
- (2) Valera-Medina, A.; Amer-Hatem, F.; Azad, A. K.; Dedoussi, I. C.; De Joannon, M.; Fernandes, R. X.; Glarborg, P.; et al. Review on ammonia as a potential fuel: from synthesis to economics. *Energy Fuels* **2021**, *35*, 6964–7029.
- (3) Han, X.; Wang, Z.; He, Y.; Liu, Y.; Zhu, Y.; Konnov, A. A. The temperature dependence of the laminar burning velocity and superadiabatic flame temperature phenomenon for  $\text{NH}_3/\text{air}$  flames. *Combust. Flame* **2020**, *217*, 314–320.
- (4) Okafor, E. C.; Naito, Y.; Colson, S.; Ichikawa, A.; Kudo, T.; Hayakawa, A.; Kobayashi, H. Experimental and numerical study of the laminar burning velocity of  $\text{CH}_4\text{-NH}_3$ -air premixed flames. *Combust. Flame* **2018**, *187*, 185–198.
- (5) Han, X.; Wang, Z.; Costa, M.; Sun, Z.; He, Y.; Cen, K. Experimental and kinetic modeling study of laminar burning velocities of  $\text{NH}_3/\text{air}$ ,  $\text{NH}_3/\text{H}_2/\text{air}$ ,  $\text{NH}_3/\text{CO}/\text{air}$  and  $\text{NH}_3/\text{CH}_4/\text{air}$  premixed flames. *Combust. Flame* **2019**, *206*, 214–226.
- (6) Li, R.; Konnov, A. A.; He, G.; Qin, F.; Zhang, D. Chemical mechanism development and reduction for combustion of  $\text{NH}_3/\text{H}_2/\text{CH}_4$  mixtures. *Fuel* **2019**, *257*, 116059.
- (7) He, X.; Shu, B.; Nascimento, D.; Moshhammer, K.; Costa, M.; Fernandes, R. X. Auto-ignition kinetics of ammonia and ammonia/hydrogen mixtures at intermediate temperatures and high pressures. *Combust. Flame* **2019**, *206*, 189–200.
- (8) Pugh, D.; Bowen, P.; Valera-Medina, A.; Giles, A.; Runyon, J.; Marsh, R. Influence of steam addition and elevated ambient conditions on  $\text{NO}_x$  reduction in a staged premixed swirling  $\text{NH}_3/\text{H}_2$  flame. *Proc. Combust. Inst.* **2019**, *37*, S401–S409.
- (9) Manna, M. V.; Sabia, P.; Ragucci, R.; de Joannon, M. Oxidation and pyrolysis of ammonia mixtures in model reactors. *Fuel* **2020**, *264*, 116768.
- (10) Sabia, P.; Manna, M. V.; Cavaliere, A.; Ragucci, R.; de Joannon, M. Ammonia oxidation features in a Jet Stirred Flow Reactor. The role of  $\text{NH}_2$  chemistry. *Fuel* **2020**, *276*, 118054.
- (11) Manna, M. V.; Sabia, P.; Ragucci, R.; de Joannon, M. Ammonia oxidation regimes and transitional behaviors in a Jet Stirred Flow Reactor. *Combust. Flame* **2021**, *228*, 388–400.
- (12) Sabia, P.; Manna, M. V.; Ragucci, R.; de Joannon, M. Mutual inhibition effect of hydrogen and ammonia in oxidation processes and the role of ammonia as “strong” collider in third-molecular reactions. *Int. J. Hydrogen Energy* **2020**, *45*, 32113–32127.
- (13) Liu, Y.; Han, D. Numerical study on explosion limits of ammonia/hydrogen/oxygen mixtures: Sensitivity and eigenvalue analysis. *Fuel* **2021**, *300*, 120964.
- (14) Liang, W.; Law, C. K. An analysis of the explosion limits of hydrogen/oxygen mixtures with nonlinear chain reactions. *Phys. Chem. Chem. Phys.* **2018**, *20*, 742–751.
- (15) Liang, W.; Liu, J.; Law, C. K. On explosion limits of  $\text{H}_2/\text{CO}/\text{O}_2$  mixtures. *Combust. Flame* **2017**, *179*, 130–137.
- (16) Liang, W.; Liu, Z.; Law, C. K. Explosion limits of  $\text{H}_2/\text{CH}_4/\text{O}_2$  mixtures: Analyticity and dominant kinetics. *Proc. Combust. Inst.* **2019**, *37*, 493–500.
- (17) Zhou, C.; Liang, W.; Yang, X.; Law, C. K. Explosion limits of hydrogen/oxygen mixtures with nitric oxide sensitization. *Fuel* **2020**, *277*, 118158.
- (18) Liang, W.; Wang, Y.; Law, C. K. Role of ozone doping in the explosion limits of hydrogen-oxygen mixtures: Multiplicity and catalyticity. *Combust. Flame* **2019**, *205*, 7–10.
- (19) Lutz, A. E.; Kee, R. J.; Miller, J. A. *SENKIN: A FORTRAN Program for Predicting Homogeneous Gas Phase Chemical Kinetics with Sensitivity Analysis*. No. SAND-87-8248; Sandia National Labs.: Livermore, CA (USA), 1988.
- (20) Wang, X.; Law, C. K. An analysis of the explosion limits of hydrogen-oxygen mixtures. *J. Chem. Phys.* **2013**, *138*, 134305.
- (21) Otomo, J.; Koshi, M.; Mitsumori, T.; Iwasaki, H.; Yamada, K. Chemical kinetic modeling of ammonia oxidation with improved reaction mechanism for ammonia/air and ammonia/hydrogen/air combustion. *Int. J. Hydrogen Energy* **2018**, *43*, 3004–3014.

- (22) Glarborg, P.; Miller, J. A.; Ruscic, B.; Klippenstein, S. J. Modeling nitrogen chemistry in combustion. *Prog. Energy Combust. Sci.* **2018**, *67*, 31–68.
- (23) Mei, B.; Zhang, X.; Ma, S.; Cui, M.; Guo, H.; Cao, Z.; Li, Y. Experimental and kinetic modeling investigation on the laminar flame propagation of ammonia under oxygen enrichment and elevated pressure conditions. *Combust. Flame* **2019**, *210*, 236–246.
- (24) Nakamura, H.; Hasegawa, S.; Tezuka, T. Kinetic modeling of ammonia/air weak flames in a micro flow reactor with a controlled temperature profile. *Combust. Flame* **2017**, *185*, 16–27.
- (25) Langer, R.; Lotz, J.; Cai, L.; vom Lehn, F.; Leppkes, K.; Naumann, U.; Pitsch, H. Adjoint sensitivity analysis of kinetic, thermochemical, and transport data of nitrogen and ammonia chemistry. *Proc. Combust. Inst.* **2021**, *38*, 777–785.